

**ARTICLE TYPE****No further evidence for a transiting inner companion to the hot Jupiter HATS-50b<sup>†</sup>**

Matthias Mallonn

<sup>1</sup>Leibniz-Institut für Astrophysik Potsdam (AIP), An der Sternwarte 16, 14482 Potsdam, Germany**Correspondence**

Email: mmallonn@aip.de

Most hot Jupiter exoplanets do not have a nearby planetary companion in their planetary system. One remarkable exception is the system of WASP-47 with an inner and outer nearby companion to a hot Jupiter, providing detailed constraints on its formation history. In this work, we follow-up on a tentative photometric signal of a transiting inner companion to the hot Jupiter HATS-50 b. If confirmed, it would be the third case of a hot Jupiter with an inner companion. 63 hours of new ground-based photometry were employed to rule out this signal to about 96 % confidence. The injection of artificial transit signals showed the data to be of sufficient quality to reveal the potential photometric feature at high significance. However, no transit signal was found. The discrete pattern of observing blocks leaves a slight chance that the transit was missed.

**KEYWORDS:**

techniques: photometric, stars: individual (HATS-50), planetary systems

**1 | INTRODUCTION**

Close-in Jupiter-sized exoplanets, the so-called hot Jupiters, are a rare phenomenon. Only about 1 percent of solar-like stars host such a planet of at least six Earth radii in size and an orbital period below 10 days (Fressin et al., 2013; Mayor et al., 2011; Wang, Fischer, Horch, & Huang, 2015). On the contrary, it is the type of exoplanets which are best characterized (Seager & Deming, 2010). This is caused by the circumstance that the hot Jupiters produce the largest signal in radial velocity and photometric measurements. Thus, most of the observational effort to characterize the atmospheres of exoplanets by emission, transmission and phase-resolved spectroscopy concentrated on these targets due to the observational feasibility (see reviews by Crossfield, 2015; Deming & Seager, 2017; Sing, 2018).

However, there are numerous unsolved questions concerning the hot Jupiters. One of these is the quest how they achieved their orbits. A review was recently

provided by Dawson & Johnson (2018). The scenarios discussed in the literature are that they either formed in situ (Batygin, Bodenheimer, & Laughlin, 2016; Bodenheimer, Hubickyj, & Lissauer, 2000; Lee & Chiang, 2016) or that they migrated inward toward their current position by interactions with the protoplanetary discs (Ida & Lin, 2008; Lin, Bodenheimer, & Richardson, 1996) or by high-eccentricity tidal migration (Ida, Lin, & Nagasawa, 2013; Wu & Lithwick, 2011).

For the majority of hot Jupiters, the high-eccentricity tidal migration presents a feasible option (Dawson & Johnson, 2018). It is broadly in agreement to the observed eccentricity distribution of hot Jupiters, and to the finding that hot Jupiters are generally alone in their close environment (Huang, Wu, & Triaud, 2016; Steffen et al., 2012). Companions orbiting the same host star have mostly been found only very far from the hot Jupiter in the outer parts of the planetary system (Knutson et al., 2014; Ngo et al., 2015), a few were found with a companion within 1 AU (Butler et al., 1999; Endl et al., 2014; Hartman et al., 2014; Wright et al., 2009). The discovery of multiple, closely packed planets in the system of WASP-47 presented a striking contrast

<sup>†</sup>Based on data obtained with the STELLA robotic telescopes in Tenerife, an AIP facility jointly operated by AIP and IAC.

(Becker, Vanderburg, Adams, Rappaport, & Schwengeler, 2015; Neveu-VanMalle et al., 2016). Next to the hot Jupiter WASP-47 b, the host star harbors two sub-Neptunes, one interior and one exterior to the hot Jupiter. The orbits of these near-by siblings would have become unstable during the high-eccentricity phase of the hot Jupiter, thus it likely formed through a different evolutionary path (Weiss et al., 2017). The only other planetary system known with an inner companion to a hot Jupiter is Kepler-730. The sub-Neptune Kepler-730 c orbits the host star with a period of 2.8 days, while the hot Jupiter Kepler-730 b has a period of 6.5 days (Cañas et al., 2019). The discovery of similar planet systems would be very valuable to learn more about the occurrence rate of such exceptional systems and their evolution.

Recently, Henning et al. (2018) announced the discovery of four hot Jupiters. In the HAT-South photometry dataset of one of them, the system of HATS-50, they found an additional signal of a transiting planet at low signal-to-noise ratio. While the hot Jupiter HATS-50 b has an orbital period of  $\sim 3.38$  days, the additional candidate signal showed a period of 0.766 days, a transit depth of 3.2 mmag, and a duration of 46 minutes. A transit fit by Henning et al. (2018) resulted in an object size larger than Neptune, with the short signal length suggesting a grazing transit. Because HATS-50 b is not grazing, but fully transiting the host star, this putative configuration of the planetary system would exhibit a mutual inclination of more than 10 degrees. The radial velocity (RV) data, obtained to confirm the planetary nature of HATS-50 b, showed substantial jitter, which might be related to the potential inner companion. No significant RV variation could be measured at the period of the photometric signal, thus Henning et al. (2018) derived an upper mass limit for the candidate HATS-50 c of  $0.16 M_J$ . The space satellite TESS (Ricker et al., 2015) would be well suited to confirm or reject the tentative transit signal. However, according to the Web TESS Viewing Tool, HATS-50 will not be observed by TESS throughout its first two years of operation.

In this work, we present our photometric follow-up campaign to verify the existence of the tentative shallow transit signal suggested by Henning et al. (2018). While the ground-based detection of the targeted small signal is clearly challenging, meter-sized ground-based telescope have proven to be capable of detecting transit and eclipse signals of milli-magnitude amplitude (e.g., Lendl et al., 2017, 2013; Mallonn et al., 2019; West et al., 2019). In Section 2, we present the new ground-based photometric observations and their data reduction. Section 3 provides the analysis of a transit signal of the hot Jupiter HATS-50 b. The analysis of the entire data set to search for the potential transiting inner companion

to the hot Jupiter is given in Section 4. We conclude our work in Section 5.

## 2 | OBSERVATIONS AND DATA REDUCTION

We obtained 63 hours of time-series photometry with the 1.2m robotic STELLA telescope and its wide field imager WiFSIP (Strassmeier et al., 2004). The instrument provides a field of view (FoV) of  $22' \times 22'$  on a scale of  $0.32''/\text{pixel}$  (Granzer, Weber, & Strassmeier, 2010). The detector is a single  $4096 \times 4096$  back-illuminated thinned CCD with  $15 \mu\text{m}$  pixels. The telescope is located on the northern hemisphere at the Canary Islands. HATS-50 is a southern target with a declination of  $-26^\circ$ . Seen from STELLA, the target is visible in the summer season for 3.5 hours at an airmass smaller than 2.0. In total, we observed blocks of 3.5 hours in 18 nights. An observing log is given in Table 1. Due to the uncertainty of the ephemeris of the suggested additional transit signal, we scheduled the observation only according to the availability of telescope time. Thus, the observations have been taken randomly in respect to the orbital phase of the putative planet.

In comparison to the population of known hot Jupiter host stars, HATS-50 is rather faint with  $V = 14$  mag. We compensated for this by an exposure time of 180 seconds for all observations, yielding an observing cadence of 223 seconds and only  $\sim 12$  data points per potential transit event. However, in average, each point in orbital phase is covered  $\sim 3$  times under the assumption of an orbital period of 0.766 days. All observations were taken in the Sloan  $r'$  filter, and we slightly defocussed the telescope to achieve more stable photometry. The average point-to-point scatter of the differential photometric light curves is 2.3 mmag.

The data reduction was done similarly to our previous analyses of exoplanet transit observations with STELLA/WiFSIP (e.g., Mallonn et al., 2016, 2015). In short, the bias and flat field correction was supplied by the official STELLA pipeline. For aperture photometry, we employed SExtractor (Bertin & Arnouts, 1996). For each individual observing night, we tested and applied the aperture size that minimized the scatter in the light curve. Also, the selection of multiple comparison stars was chosen nightly to minimize the scatter. As the last step of the extraction of the differential light curves, we applied a  $4 \sigma$  clipping to the nightly data to remove outliers.

## 3 | TIMING OF THE TRANSIT OF HATS-50 B

During the first observing block, a partial transit of HATS-50 b was observed by chance. Its light curve is shown in Figure 1.

<sup>0</sup><https://heasarc.gsfc.nasa.gov/cgi-bin/tess/webtess/wtv.py>

**TABLE 1** Overview of observations of HATS-50 taken with the STELLA telescope in the Sloan r' filter. The columns provide the observing date, the number of the observed individual data points, the exposure time, the dispersion of the data points as root-mean-square (rms), and the airmass range of the observations.

Date	$N_{\text{data}}$	rms (mmag)	Airmass
2018-06-09	56	1.7	1.71 - 2.10
2018-06-10	56	2.3	1.71 - 2.08
2018-06-13	57	2.2	1.71 - 2.02
2018-06-14	53	2.4	1.71 - 1.98
2018-06-16	56	2.0	1.71 - 2.02
2018-06-17	56	1.9	1.71 - 2.05
2018-08-29	57	2.4	1.71 - 2.14
2018-08-30	57	2.5	1.71 - 2.10
2018-09-01	57	2.8	1.71 - 2.15
2018-09-03	57	2.8	1.71 - 2.10
2018-09-04	56	2.3	1.71 - 2.08
2018-09-06	57	2.3	1.71 - 2.03
2018-09-07	56	2.4	1.71 - 2.02
2018-09-08	57	2.0	1.71 - 2.00
2018-09-09	57	2.9	1.71 - 1.99
2018-09-10	57	2.2	1.71 - 1.99
2018-09-11	57	2.0	1.71 - 2.01
2018-09-16	57	2.1	1.71 - 2.10

We derive the mid time of the transit and provide it here for any future parameter and ephemeris refinement work on this hot Jupiter.

The transit analysis is done with the publicly available software tool JKTEBOP (Southworth, 2008; Southworth, Maxted, & Smalley, 2004). The transit model involves the fit parameters of the orbital semi-major axis scaled by the stellar radius  $a/R_*$ , the orbital inclination  $i$ , the planet-star radius ratio  $k$ , the mid point of the transit  $T_0$ , the orbital period  $P$ , the eccentricity of the orbit  $e$ , the argument of periastron  $\omega$ , and detrending coefficients  $c_{0,1}$ . For detrending, we chose a linear function over time which was found to minimize the Bayesian Information Criterion (BIC, Schwarz, 1978). This choice is in agreement to Mackebrandt et al. (2017), who also found a first order polynomial as best choice for the detrending of photometric WiFSIP data of about three hours duration. We re-scaled the photometric uncertainties to match the point-to-point dispersion in the light curve (see Section 4). The limb darkening coefficients of the quadratic limb darkening law for the Sloan r' band were adopted from Henning et al. (2018).

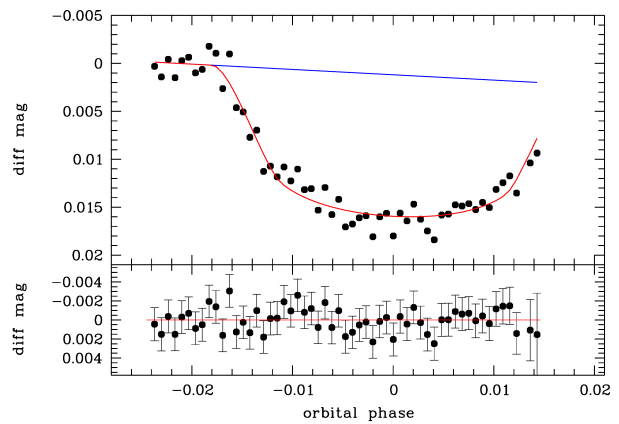


**FIGURE 1** Transit light curve of the hot Jupiter HATS-50 b. Upper panel: the red solid line shows the transit plus linear trend model, the blue solid lines shows only the linear trend. Black data points denote the STELLA observations. Lower panel: black data points show the light curve residuals after subtraction of the transit plus linear trend model.

Since we provide in this work only one new partial transit observation of HATS-50 b, we do not intend to refine transit parameters like  $a/R_*$  or  $i$ . Thus, we fix all fit parameters to the values derived in Henning et al. (2018), and fit the light curve for the transit timing  $T_0$  and the two detrending coefficients.

The resulting transit mid time of the hot Jupiter HATS-50 b is  $2458279.67541 \pm 0.0018$  (BJD<sub>TDB</sub>), which is in  $1.3\sigma$  agreement to the ephemeris of Henning et al. (2018), if the uncertainties of the timing measurement and the ephemeris are quadratically combined. We subtracted the transit model of HATS-50 b for further analysis from the light curve of the first observing block. No other data set of our sample was affected by a transit of the hot Jupiter.

## 4 | ANALYSIS AND RESULTS

Before we search for a transit signal of an inner companion to HATS-50 b in the data, we tested different parametric detrending functions and used the BIC to select the best. We compared linear combinations of low-order polynomials with time, airmass, object FWHM, and x and y position on the chip as independent variables. As in Section 3 for the first observing block, we found the very simple first-order polynomial over time to minimize the BIC also for all other observing blocks.

In the next step, we re-scale the individual photometric uncertainties. The values derived from SExtractor tend to underestimate the errors, since they only account for the photon noise of target and comparison star and their respective

background. We inflate the individual photometric uncertainties by a common factor such that the light curves per observing block reach a reduced  $\chi^2$  of unity versus the detrending function.

#### 4.1 | Initial transit fit

To search for a transit signal of an inner companion to HATS-50b, first we perform a transit fit with JKTEBOP. In one attempt, we fit for all relevant parameters  $a/R_*$ ,  $i$ ,  $k$ ,  $P$ ,  $T_0$ , and two detrending coefficients per observing block. The two limb darkening coefficients of the quadratic limb darkening law were fixed to the values of Henning et al. (2018), and for simplicity we fixed the eccentricity of the potential planet  $e$  to zero. In another attempt, we first created a transit model that produced a grazing transit with  $10^\circ$  mutual inclination to HATS-50b and a transit depth and duration as suggested by Henning et al. (2018), and then fixed  $a/R_*$  and  $i$  to the values of this model, leaving all other parameters free. In both fit versions, we used the values of Henning et al. (2018) for  $P$  and  $T_0$  as initial parameter values. Then, in additional fit runs, we moved the initial  $T_0$  through the orbital phase in steps of 0.2. In no case we detected a transit feature similar to the tentative transit detection of Henning et al. (2018). The best fit models had transit depths of 1 mmag or smaller which were always in agreement to a depth of zero within  $2\sigma$  or less. The BIC values of the models with a transit were larger than the BIC values of a model only including detrending, thus the no-transit models were favored. Also, a visual inspection provided no indication for a transit feature of about 3 mmag depth.

We can already conclude at this stage of our work that we cannot confirm the suggested transit signal with our new STELLA photometry. The remaining part of our work will be devoted to the question whether we can rule out this signal significantly.

#### 4.2 | Recovery of an injected transit signal

We will investigate whether the new STELLA photometry is of sufficient quality to reveal a transit signal as suggested by Henning et al. (2018). For this purpose, we create a transit model of 46 minutes duration and a depth of 3.2 mmag with JKTEBOP and inject it into our observing data. We apply the suggested orbital period of 0.7662482 days and the timing zero point of  $T_c = 2455274.38586$ . Afterwards, we move the injected transit signal through orbital phase in steps of 0.2, hence we repeat the exercise of signal recovery five times. The radius ratio  $k$  of the injected transit was 0.06, and in all five cases, we recovered this value well with values ranging from 0.057 to 0.066 and an uncertainty range from 0.004 to 0.006.

In all five cases, the BIC values favored the model including the transit.

#### 4.3 | A simple box model for the transit search

In the previous sections of this work, we have demonstrated that our data are of sufficient quality to reveal a transit feature of suggested depth, duration, and periodicity. However, the ability to reveal a photometric transit signal obviously depends on the orbital phase coverage. This phase coverage might not be complete for certain orbital periods. To investigate on the question whether our data rule out the 3 mmag transit feature for a range of orbital periods around the suggested value, we compare the BIC values of the transit-plus-detrending model versus the detrending-only model for a large number of combinations of  $P$  and  $T_0$ . We consider a transit model to be rejected if its BIC value is larger by a difference of 10 than the corresponding detrending-only model. To save computational time, we approximate the transit signal with a simple box model. Because of the potentially grazing shape of the transit (Henning et al., 2018), we design a box of 46 minutes length, but a more shallow depth of 2.5 mmag instead of the suggested depth of 3.2 mmag. We chose a certain value for the orbital period and move the box through the orbital phase in steps of 0.01 (which corresponds to 11 minutes for a period of 0.766 days).

We consider a period range of  $\pm 5\%$  of the suggested period as wide and exhaustive for our exercise, since the typical period uncertainty of a transiting, ground-based detected planet is  $\ll 0.01\%$ , however typically with substantially more follow-up observations. Thus, we examine a period range from 0.729 to 0.804 days in steps of 0.0001 days.

The result is a distribution of BIC differences for each period-phase combination. The first outcome was that in no case, such difference between transit-plus-detrending and detrending-only model was below -10, i.e. in no case the transit model was significantly favored. On the other side, the transit feature was not ruled out in 100% of the period-phase combinations, which means there are cases with a BIC difference of below 10 and no model was significantly favored over the other. We inspected examples of these near-zero BIC differences and found them all to be associated to an incomplete orbital phase coverage caused by our irregular sequence of observing blocks. In Figure 2, we show in the upper panel the STELLA data phase folded to the period of 0.766428 suggested by Henning et al. (2018). In the middle panel, we show a randomly drawn example of a period for which we have full phase coverage. For such period, the transit feature is ruled out at all phases. In the lower panel of Figure 2, we give an example of an orbital period close to the suggested value, for which our data cannot rule out the transit feature completely

because the phase coverage is not complete. Potentially, we could have missed the transit with our observations and it could be hidden in the phase gap.

For the examined combinations of orbital period and phase from  $P = 0.729$  to  $P = 0.804$ , we obtain a BIC value larger than 10 in 95.9% of all cases. That means that there is a slight probability of  $\sim 4\%$  that we have missed the transit. Hence, we can rule the transit feature out to about 96% confidence. The value remains very similar for a period range tighter around the suggested period and varies from 95.5% to 96.5% dependent on the specific period interval.

## 5 | DISCUSSION AND CONCLUSION

We presented 63 hours of follow-up photometry of HATS-50 to verify a transiting feature of an inner companion to the hot Jupiter HATS-50 b, which was tentatively detected by Henning et al. (2018). The existence of an inner or nearby outer companion to a hot Jupiter is informative of its formation and evolution, since the three theoretically most discussed formation scenarios make distinct predictions. In situ formation can form nearby planets outside of orbital resonances, disk migration scenarios result in nearby resonant companions, and high-eccentricity migration eliminates nearby companions (Dawson & Johnson, 2018). Observational evidence have shown that the vast majority of hot Jupiters does not have nearby companions (Huang et al., 2016; Latham et al., 2011; Steffen et al., 2012). Constraints on the evolutionary history come from statistical properties of their population rather than from individual planet systems. On the contrary, the only planetary systems found with an inner companion to a hot Jupiter so far, WASP-47 and Kepler-730, already allowed conclusions on their evolution based on the individual planetary parameters. For example, Weiss et al. (2017) described that none of the three formation scenarios mentioned above, in situ formation, disk migration, and high-eccentricity migration, can produce all the physical properties of the WASP-47 system. Instead, it is more likely that the system underwent multiple stages of planet formation with individual planets formed at different times.

The discovery of other nearby companions to hot Jupiters or a tight constraint on their existence would therefore be of great interest for our understanding of hot Jupiter formation. Our new photometric data set of HATS-50 could not confirm the existence of the suggested transiting inner companion to HATS-50 b, though the injection and recovery of artificial transit signals proved the data to be of sufficient photometric quality. We ruled out the existence of the suggested transit feature to 96% confidence, leaving the slight possibility that we missed the transit due to our discrete observing pattern of many observing blocks. This pattern causes an incomplete

phase coverage for a small fraction of the examined orbital period interval. Space-based observatories like Spitzer, TESS, or CHEOPS could deliver the continuous observation of a full planet orbit without phase gaps typical for ground-based observatories to rule out an inner transiting companion at even higher confidence.

## ACKNOWLEDGMENTS

We thank Carolina von Essen and Katja Poppenhaefer for helpful discussions on the manuscript. We thank Thomas Granzer for technical support with the STELLA observations. This work made use of the SIMBAD data base and VizieR catalog access tool, operated at CDS, Strasbourg, France, and of the NASA Astrophysics Data System (ADS).

## REFERENCES

- Batygin, K., Bodenheimer, P. H., & Laughlin, G. P. 2016, October, *ApJ*, 829, 114. doi:
- Becker, J. C., Vanderburg, A., Adams, F. C., Rappaport, S. A., & Schwengeler, H. M. 2015, October, *ApJ*, 812, L18. doi:
- Bertin, E., & Arnouts, S. 1996, Jun, *A&AS*, 117, 393-404. doi:
- Bodenheimer, P., Hubickyj, O., & Lissauer, J. J. 2000, January, *Icarus*, 143, 2-14. doi:
- Butler, R. P., Marcy, G. W., Fischer, D. A. et al. 1999, Dec, *ApJ*, 526(2), 916-927. doi:
- Cañas, C. I., Wang, S., Mahadevan, S. et al. 2019, Jan, *ApJ*, 870(2), L17. doi:
- Crossfield, I. J. M. 2015, October, *PASP*, 127, 941. doi:
- Dawson, R. I., & Johnson, J. A. 2018, September, *ARA&A*, 56, 175-221. doi:
- Deming, D., & Seager, S. 2017, *JGRE*, 122, 2169-9097.
- Endl, M., Caldwell, D. A., Barclay, T. et al. 2014, November, *ApJ*, 795, 151. doi:
- Fressin, F., Torres, G., Charbonneau, D. et al. 2013, April, *ApJ*, 766, 81. doi:
- Granzer, T., Weber, M., & Strassmeier, K. G. 2010, *Advances in Astronomy*, 2010, 980182. doi:
- Hartman, J. D., Bakos, G. Á., Torres, G. et al. 2014, Jun, *AJ*, 147(6), 128. doi:
- Henning, T., Mancini, L., Sarkis, P. et al. 2018, February, *AJ*, 155, 79. doi:
- Huang, C., Wu, Y., & Triaud, A. H. M. J. 2016, July, *ApJ*, 825, 98. doi:
- Ida, S., & Lin, D. N. C. 2008, January, *ApJ*, 673, 487-501. doi:
- Ida, S., Lin, D. N. C., & Nagasawa, M. 2013, September, *ApJ*, 775, 42. doi:
- Knutson, H. A., Fulton, B. J., Montet, B. T. et al. 2014, April, *ApJ*, 785, 126. doi:
- Latham, D. W., Rowe, J. F., Quinn, S. N. et al. 2011, May, *ApJ*, 732(2), L24. doi:
- Lee, E. J., & Chiang, E. 2016, February, *ApJ*, 817, 90. doi:
- Lendl, M., Ehrenreich, D., Turner, O. D. et al. 2017, Jul, *A&A*, 603, L5. doi:
- Lendl, M., Gillon, M., Queloz, D., Alonso, R., Fumel, A., Jehin, E., & Naef, D. 2013, Apr, *A&A*, 552, A2. doi:

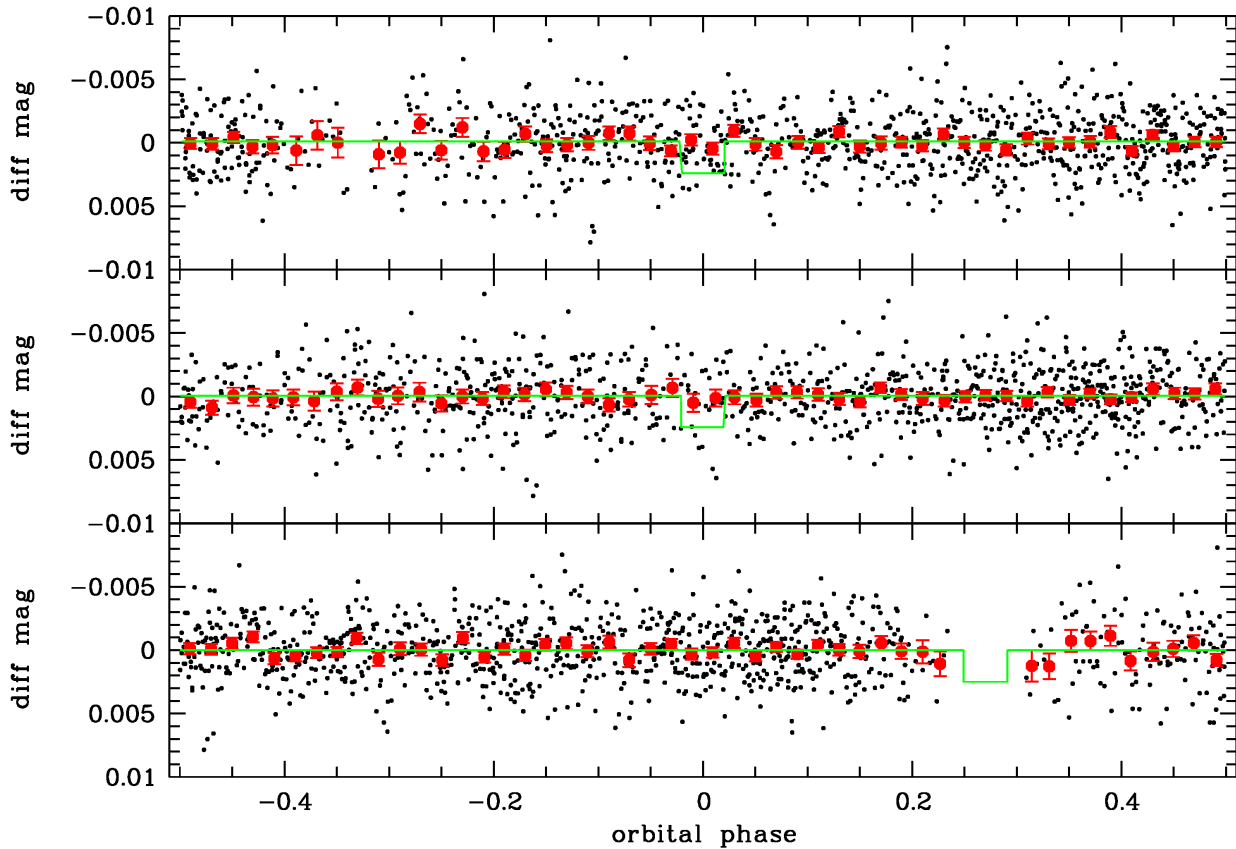


**FIGURE 2** Phase-folded STELLA photometry. Upper panel: Shown are the observing data in black folded to the suggested period of  $P = 0.766248$  days. In red, the data are binned in steps of 0.05 in phase. The box model of 46 minutes length and 2.5 mmag depth is shown in green, centered on the transit mid time suggested by Henning et al. (2018). Middle panel: The data are phase-folded to a period with complete phase coverage, here  $P = 0.7670$  days. The transit feature can be ruled out for all orbital phases. Lower panel: An example of a period with incomplete phase coverage, here  $P = 0.7656$  days, is given. The transit feature is ruled out for all orbital phases covered with observations, however, the feature might potentially be hidden in the phase gap, as illustrated by the green model.

- Lin, D. N. C., Bodenheimer, P., & Richardson, D. C. 1996, April, *Nature*, 380, 606-607. doi:
- Mackebrandt, F., Mallonn, M., Ohlert, J. M. et al. 2017, December, *A&A*, 608, A26. doi:
- Mallonn, M., Bernt, I., Herrero, E. et al. 2016, November, *MNRAS*, 463, 604-614. doi:
- Mallonn, M., Köhler, J., Alexoudi, X., von Essen, C., Granzer, T., Poppenhaeger, K., & Strassmeier, K. G. 2019, Apr, *A&A*, 624, A62. doi:
- Mallonn, M., Nascimbeni, V., Weingrill, J. et al. 2015, November, *A&A*, 583, A138. doi:
- Mayor, M., Marmier, M., Lovis, C. et al. 2011, September, *arXiv e-prints*.
- Neveu-VanMalle, M., Queloz, D., Anderson, D. R. et al. 2016, February, *A&A*, 586, A93. doi:
- Ngo, H., Knutson, H. A., Hinkley, S. et al. 2015, Feb, *ApJ*, 800(2), 138. doi:
- Ricker, G. R., Winn, J. N., Vanderspek, R. et al. 2015, Jan, *Journal of Astronomical Telescopes, Instruments, and Systems*, 1, 014003. doi:
- Schwarz, G. 1978, April, *Annals of Statistics*, 6, 461-464.
- Seager, S., & Deming, D. 2010, September, *ARA&A*, 48, 631-672. doi:
- Sing, D. K. 2018, April, *arXiv e-prints*.
- Southworth, J. 2008, May, *MNRAS*, 386, 1644-1666. doi:
- Southworth, J., Maxted, P. F. L., & Smalley, B. 2004, July, *MNRAS*, 351, 1277-1289. doi:
- Steffen, J. H., Ragozzine, D., Fabrycky, D. C. et al. 2012, May, *Proceedings of the National Academy of Science*, 109, 7982-7987. doi:
- Strassmeier, K. G., Granzer, T., Weber, M. et al. 2004, October, *Astronomische Nachrichten*, 325, 527-532. doi:
- Wang, J., Fischer, D. A., Horch, E. P., & Huang, X. 2015, February, *ApJ*, 799, 229. doi:
- Weiss, L. M., Deck, K. M., Sinukoff, E. et al. 2017, Jun, *AJ*, 153(6), 265. doi:

- West, R. G., Gillen, E., Bayliss, D. et al. 2019, Jul, *MNRAS*, 486(4), 5094-5103. doi:
- Wright, J. T., Fischer, D. A., Ford, E. B. et al. 2009, Jul, *ApJ*, 699(2), L97-L101. doi:
- Wu, Y., & Lithwick, Y. 2011, July, *ApJ*, 735, 109. doi:

